Plant Physiology and Biochemistry 142 (2019) 22–33

Contents lists available at ScienceDirect

Plant Physiology and Biochemistry

journal homepage: www.elsevier.com/locate/plaphy

Research article

Metabolite and gene expression analysis reveal the molecular mechanism for petal colour variation in six *Centaurea cyanus* cultivars

Chengyan Deng[a], Shanshan Li[b,c], Chengyong Feng[b,c], Yan Hong[a], He Huang[a], Jiaying Wang[a], Liangsheng Wang[b,c,**], Silan Dai[a,*]

[a] Beijing Key Laboratory of Ornamental Plants Germplasm Innovation & Molecular Breeding, National Engineering Research Center for Floriculture, Beijing Laboratory of Urban and Rural Ecological Environment and College of Landscape Architecture, Beijing Forestry University, Beijing, 100083, China
[b] Key Laboratory of Plant Resources and Beijing Botanical Garden, Institute of Botany, The Chinese Academy of Sciences, Beijing, 100093, China
[c] University of Chinese Academy of Sciences, Beijing, 100049, China

ARTICLE INFO

Keywords:
Centaurea cyanus
Petal colour
Flavonoids
Gene expression
Biosynthetic pathway

ABSTRACT

Centaurea cyanus is a popular garden plant native to Europe. Although their petals show abundant colour variations, the flavonoid profiling and the potential molecular mechanisms remain unclear. In the present study, we collected six cornflower cultivars with white, pink, red, blue, mauve and black petals. Ultra-performance liquid chromatography coupled with photodiode array and tandem mass spectrometry (UPLC-MS/MS) was used to investigate the comparative profiling of flavonoids both qualitatively and quantitatively. Ten anthocyanins, six flavones and two flavonols were separated and putatively identified. Except for white petals without any anthocyanins, both pink and red flowers contained pelargonidin derivatives, whereas blue, mauve and black petals accumulated cyanidins. The expression patterns of genes involved in the flavonoid biosynthesis were performed by real-time quantitative reverse transcription-PCR. The anthocyanin biosynthetic pathway in white petals was inhibited starting from flavanone 3-hydroxylase, resulting in the absence of anthocyanin accumulation. The open reading frame of flavonoid 3′-hydroxylase in pink and red petals was truncated; this led to loss of a haem binding site, a conserved motif in the cytochrome P450 family, and loss of conversion from dihydrokaempferol to dihydroquercetin. The significantly higher expression of structural genes corresponding to the hyper-accumulation of flavonoids in black petals may play an important role in black coloration. Remarkably, the mauve and blue petals accumulated the same cyanidin derivative but contained apigenin with different modifications on the 4′ position, which may cause the coloration differences. The results obtained in this study will provide insights into the mechanisms of vivid colour diversities in cornflower.

1. Introduction

Flower colour is one of the most attractive traits in ornamental plants. Many factors influence colour development, including pigments, vacuolar pH, metal ion, and the structure of epidermal cells (Zhao and Tao., 2015). Flavonoids are secondary metabolites that exist in plants. They can further be divided into anthocyanin, flavone, flavonol, flavanone, flavanol and isoflavone (Tohge et al., 2017). Anthocyanin is an important subclass that enables plants with vivid colours to attract pollinators and seed dispersers and receive protection from salt, light or drought stress (Lotkowska et al., 2015; Li et al., 2017). The common anthocyanins are derivatives of cyanidin, pelargonidin, delphinidin, petunidin, peonidin, primulagenidin and malvidin. The anthocyanins that accumulate in plant petals mainly determine the colour variation among species and cultivars. Generally, delphinidin gives petals a vivid blue colour, such as that seen in *Senecio cruentus* and *Delphinium grandiflorum* (Jin et al., 2016; Ishii et al., 2017). Pelargonidin derivatives make petals show an orange-red colour, such as that seen in orange *Euphorbia pulcherrima* and transgenic *Petunia* × *hybrida* (Haselmair-Gosch et al., 2018; Nitarska et al., 2018). The cyanidin derivatives commonly facilitate pink to red colours in flowers of *Chrysanthemum morifolium* and *Lilium* spp. (Hong et al., 2015; Suzuki et al., 2016), whereas cyanidin in cornflower and *Meconopsis grandis* express vivid blue colours (Yoshida and Negishi, 2013; Yoshida et al., 2006); this discrepancy attracts great attention from researchers that seek to explore the underlying mechanisms.

* Corresponding author. Beijing Forestry University, Beijing 100083, China.
** Corresponding author. Key Laboratory of Plant Resources and Beijing Botanical Garden, Institute of Botany, The Chinese Academy of Sciences, Beijing, 100093, China.
E-mail address: silandai@sina.com (S. Dai).

https://doi.org/10.1016/j.plaphy.2019.06.018
Received 19 April 2019; Received in revised form 9 June 2019; Accepted 13 June 2019
Available online 14 June 2019

Centaurea cyanus L., is an annual or biennial plant native to Europe with attractive capitulums. Researchers have bred diverse cultivars with white, pink, red, mauve and black colours, which make it an ideal subject to investigate flower colour development. The phenomenon that cornflowers with cyanidins show bright blue colour arouses great interest in researchers. Tamura et al. (1983) reported the pigments in blue cornflower were cyanidin-3-*O*-(6″-*O*-succinyl-*β*-D-glucoside)-5-*O*-*β*-D-glucoside and apigenin-4′-*O*-(6-*O*-malonyl-*β*-D-glucoside)-7-*O*-D-glucuronide. The X-ray structural determination of the protocyanin crystal showed the supramolecular pigment composed of six cyanins, six apigenins, one ferric ion, one magnesium and two calcium ions (Shiono et al., 2005). Previous studies have examined blue colour development in cornflowers. However, the mechanisms of colour variation in *C. cyanus* remain unclear.

In this study, we used UPLC-MS/MS to isolate and identify flavonoids in six cornflower cultivars with visibly different colours. Furthermore, the expression patterns of structural genes were analysed to better understand the branch pathway of flavonoid biosynthesis. The results obtained in this study will enhance our understanding of the mechanisms associated with colour diversity in cornflower.

2. Materials and methods

2.1. Plant material

The seeds of *C. cyanus* 'Dwarf Tom Pouce White/Pink/Red/Blue' and 'Tall Double Ball Mauve/Black' were purchased from the Outsidepride Seed Company. The white, pink, red, blue, mauve and black cultivars were named DTPW, DTPP, DTPR, DTPB, TDBM and TDBB, respectively. There are four stages in the development of the cornflower capitulums: S1, the petals were colourless and embedded in bracts; S2, the petals emerged out of the bracts and the colour part occupied less than 50 percent of the whole; S3, the petals outgrew the bracts and were in full colour; S4, the petals opened and the angle between the petals and the stem was approximately 90°(Fig. 1). The petals of S4 were collected, dried in the vacuum freeze drier under −45 °C for 24 h, powdered and subpackaged in 10 ml tubes with 0.1 g for flavonoid analysis. All stages of the fresh petals were collected and stored at −80 °C for RNA extraction. The royal horticultural society colour chart (RHSCC) and colorimeter (Avantes AvaSpec-2048 L, Netherlands) were used to describe the colour phenotypes of petals in S4. Five random measurements were made for each sample and the mean value was used for analysis.

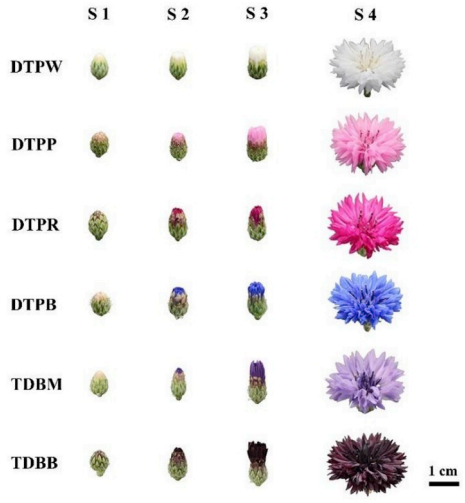

Fig. 1. Cornflower cultivars with different petal colors and their developmental stages. (For interpretation of the references to colour in this figure legend, the reader is referred to the Web version of this article.)

2.2. Standards and reagents

Cyanidin-3,5-di-*O*-glucoside (Cy3G5G) and quercetin 3-*O*-rutinoside (rutin) were purchased from the Sigma-Aldrich (St. Louis, USA) and the National Institute for the Control of Pharmaceutical and Biological Products (Beijing, China), respectively. The analytical grade solvents methanol (CH_3OH) and formic acid (HCOOH) were purchased from Beijing Chemical Works (Beijing, China). Acetonitrile of chromatographic grade used for extraction and ultra-performance liquid chromatography/triple quadrupole mass spectrometry (I-Class UPLC/Xevo™ TQ MS) analysis was purchased from Alltech Scientific (Beijing, China). HPLC-grade water was purified by a Mill-Q Water Purification system (Millipore, MA, USA).

2.3. Preparation of standard solutions and extraction of flavonoids

Standards of Cy3G5G and rutin were accurately weighed, dissolved in 0.2% HCOOH/CH_3OH (0.2/100, v/v) and CH_3OH/H_2O (70/30, v/v), respectively, and then diluted to a series of concentrations, between 31.25 and 500 μg/mL, to establish calibration curves at 525 and 350 nm, respectively. The above dried petal powder was extracted with CH_3CN/H_2O (1:1, v:v) containing 0.5% formic acid. All supernatants were collected and passed through 0.22 μm reinforced nylon membrane filters (Shanghai ANPEL, Shanghai, China) before I-Class UPLC/Xevo™ TQ MS analysis. Three replicates were performed for each treatment.

2.4. Ultra performance liquid chromatography analysis and MS spectrometry analysis conditions

Flavonoids were separated by a 10 cm × 2.1 mm Waters® ACQUITY™ 1.7 μm BEH C18 column (Waters, Milford, MA, USA) using a Waters ACQUITY Ultra Performance Liquid Chromatograpm system (UPLC I-CLASS, Waters). The column temperature was set at 35 °C and photodiode array spectra were recorded from 200 to 800 nm. The analysis was achieved with gradient elution using water containing 0.1% formic acid (solvent A) and CH_3CN (solvent B) as the mobile phase at a flow rate of 0.4 mL/min. Gradient conditions for the mobile phase were as follows: 5% B at 0 min, 45% B at 6 min, 90% B at 7 min, 5% B at 7 min 10 s, 5% B at 10 min. The injection volume for each sample was 1 μL. The peaks for anthocyanins and other flavonoids were traced at 525 and 350 nm, respectively.

The qualitative analysis of flavonoids was performed using a Xevo™ TQ-MS triple quadrupole mass spectrometer (Waters, Milford, MA, USA) connected to an ACQUITY Ultra Performance Liquid Chromatogram (UPLC I-CLASS, Waters). The ionization was achieved using an ESI source both in positive ion (PI) and negative ion (NI) mode. The ionization source parameters were set as follows: capillary voltage, 3.50(+)/3.0(-); cone voltage, 50 v; desolvation gas flow, 800 L/h; cone gas flow, 50 L/h; collision gas flow, 0.16 (+)/0.15 (-) mL/min; collision energy, 15(+)/22(-) eV; desolvation temperature, 400 °C; source temperature, 150 °C; and scan range, 50–1000(m/z) units. Analytical software (MassLynx, version 4.1) was used for the system control and data processing.

2.5. Quantitative and qualitative analysis

The content of flavonoids in acetonitrile extracts was quantified by UPLC analysis with detection wavelength 525 nm for anthocyanins and at 350 nm for other flavonoids based on the calibration curves obtained from the dilution series of Cy3G5G and rutin, respectively. The regression equations were Y = 49915 X+134.58 (R^2 = 0.9998) and Y = 103594 X-501.38 (R^2 = 0.9942) for rutin and Cy3G5G, respectively, showing good linearity between concentration and peak areas. The results were expressed in milligrams of Cy3G5G equivalents for anthocyanins and of rutin equivalents for other flavonoids per gram of dry weight (mg·g^{-1} DW).

Table 1
The petal colour phenotypes of six cornflower cultivars.

Cultivars	RHSCC code	Color group	CIE $L^*a^*b^*$				
			L^*	a^*	b^*	h	C^*
DTPW	155 D	White	93 ± 1.2 a	−1.5 ± 0.5 c	5.4 ± 0.9 a	105.7 ± 5.6 c	5.6 ± 0.8 d
DTPP	65 A	Red-purple	69.7 ± 7.1 b	34.3 ± 9.5 b	−10 ± 2.8 c	343.6 ± 4.5 a	35.8 ± 9.4 c
DTPR	N66 A	Red-purple	39.2 ± 8 d	48 ± 2 a	−10.6 ± 1.6 c	347.3 ± 2.5 a	49.3 ± 1.6 b
DTPB	100 B	Blue	55.9 ± 10.6 c	29.4 ± 3 b	−55.4 ± 0.8 e	297.9 ± 2 b	62.8 ± 2.1 a
TDBM	92 B	Violet-blue	68.1 ± 3.1 b	28.6 ± 7.1 b	−25.6 ± 2.6 d	317.7 ± 4.1 ab	38.5 ± 7.1 c
TDBB	187 A	Greyed-purple	19.1 ± 1 e	35.9 ± 1.2 b	−2.5 ± 0.7 b	332 ± 40.6 a	36 ± 1.1 c

Note: Duncan's multiple test. Different lower-case letters indicate significant difference at 5% level.

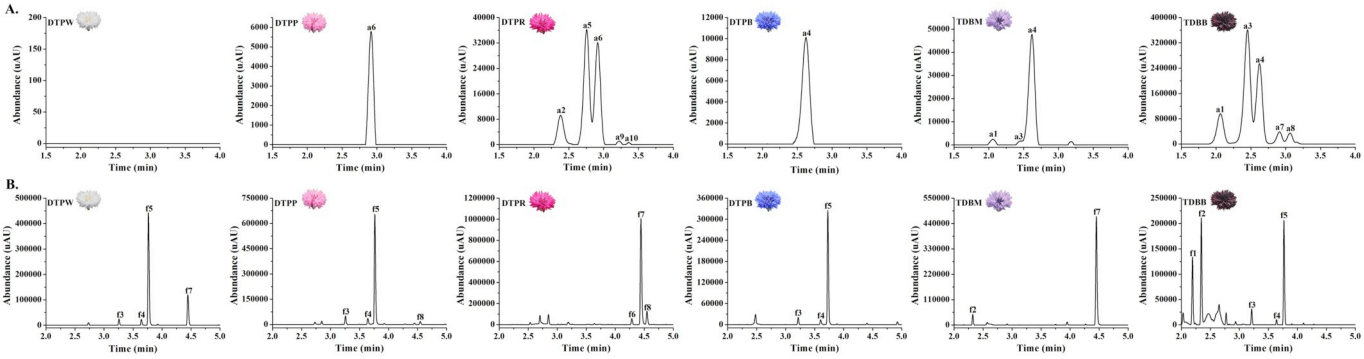

Fig. 2. The UPLC chromatograms of petal extracts of cornflower cultivars. A. Anthocyanins detected at 525 nm (see Table 2 for identification of numbered peaks); B. The other flavonoids detected at 350 nm (see Table 3 for identification of numbered peaks).

Anthocyanins and other flavonoids were identified according to their UPLC retention times, elution order, UV–vis spectra and MS data by comparison with standards and published data. Special attention was given to MS fragmentation characteristics to identify the molecular weight and position of the link between aglycone and sugar.

2.6. The isolation, expression and sequence analysis of genes involved in flavonoid biosynthesis

Total RNA of six cultivars and 4 developmental stages were isolated using the Quick RNA Isolation Kit (Huayueyang Biotechnology Co. Ltd., Beijing, China). First-strand cDNA was generated by using M-MLV reverse transcriptase (Promega, Germany). Real-time quantitative reverse transcription-PCR (RT-qPCR) was performed for gene expression analysis using a Mini Opticon Real-time PCR System (Bio-Rad Laboratories Inc., Hercules, CA, USA) based on the SYBR Premix Ex Taq (Takara Bio Inc., Shiga, Japan) with three replicates. Most genes involved in flavonoid biosynthesis were obtained from the transcriptome information from DTPB (unpublished), including *PAL*(MK732536), 4CL (MK732537), *CHS1*(KY606304), *CHS2*(MK732538), *CHS3*(MK732539), *CHI1*(MK732540), *CHI2*(MK732541), *FNS*(MK732542), *F3H* (MK732543), *DFR*(MK732544), *ANS*(MK732545), *GT1*(MK732546), *GT2*(MK732547), *GT3*(MK732548), *AT1*(MK732549) and *AT2*(MK732550). Besides, the gene sequence information of *F3′H* (FJ753550) were obtained from Genebank. The cornflower actin (KY621346.1) was used as an internal control gene. The 3′-rapid amplification of cDNA ends (3′-RACE) was used to isolate the *F3′H* (MK952786) from DTPP and DTPR. The PCR product was cloned into the pCloneEZ-TOPO vector and confirmed by sequencing. The primers for RT-qPCR and 3′-RACE were shown in Table S1. DNAMAN 9.0 was used to perform multiple sequence alignment. All the genes above were released in Genebank and the assigned numbers were shown in brackets following the gene names, respectively.

2.7. Statistical analysis

The software Masslynx 4.1 was used to analyse UPLC-MS/MS data. The data processing was performed using Excel 2010 and SPSS 20.0. Photographs were created using Origin 8.0 and Chemdraw 15.0.

3. Results

3.1. Description of flower colour phenotypes

DTPP and DTPR belong to the red-purple group, whereas DTPW, DTPB, TDBM, and TDBB were divided into the white, blue, violet-blue and greyed-purple groups, respectively. The colour coordinate values showed significant differences across cultivars. The L^*, which ranged from 19.1 to 93, was highest in DTPW; this was almost five times higher than TDBB. The a^*, which indicates redness, was highest in DTPR. The b^*, which ranged from −55.4 to 5.4, showed the most significant difference among cultivars. The petals of DTPB possessed the highest C^* value, followed by DTPR (Table 1).

3.2. Identification of anthocyanins

Anthocyanins extracted from petals of six cornflower cultivars in acidic acetonitrile solution were identified using UPLC-MS/MS. The typical UPLC chromatogram of the extracts at 525 nm showed ten peaks (Fig. 2A) with characteristic spectra of anthocyanins; these were numbered based on their elution time and identified by the characteristics of UV–vis absorption spectroscopy combined with mass spectrum data (Table 2). Their chemical formulas were shown visually in Fig. 3A.

Peaks **a1**, **a3**, **a4**, **a7** and **a8** had similar absorption spectrums and showed the same aglycon ions at m/z 287$[Y_0]^+$, which was a typical characteristic of cyanidin. The glycosylation of anthocyanins is reported to occur at 3 and 5 positions and the acylation of anthocyanidin-3-*O*-glucosides preceded 5-*O*-glucosylation in *Centaurea* (Tamura et al.,

Table 2
Putative identification of anthocyanins in petals of cornflower cultivars by I-Class UPLC/Xevo™ TQ MS.

Peak No.	Tr(min)	λ_{max}(nm)	ESI(+)	Putative identification	References
a1	2.08	238, 278, 514	611[M]$^+$(24),449[M-162]$^+$(20),287[Y_0]$^+$(100)	Cyanidin-3-*O*-glucoside-5-*O*-glucoside	Standard
a2	2.38	229,277,499	711[M]$^+$(19),595[M-116]$^+$(94),549[M-162]$^+$(13),433[M-(162 + 116)]$^+$(100),271[Y_0]$^+$(97)	Pelargonidin-3-*O*-malyl-glucoside-5-*O*-glucoside	
a3	2.47	237,277,516	697[M]$^+$(53),535[M-162]$^+$(84),449[M-(162 + 86)]$^+$(4),287[Y_0]$^+$(100)	Cyanidin-3-*O*-malonyl-glucoside-5-*O*-glucoside	
a4	2.64	232,278,516	711[M]$^+$(100),611[M-100]$^+$(5),549[M-162]$^+$(19),449[M-(162 + 100)]$^+$(9),287[Y_0]$^+$(20)	Cyanidin-3-*O*-(6″-*O*-succinyl-glucoside)-5-*O*-glucoside	Tamura et al. (1983)
a5	2.76	228,277,499	681[M]$^+$(100),595[M-86]$^+$(14),519[M-162]$^+$(43),433[M-(162 + 86)]$^+$(19),271[Y_0]$^+$(34)	Pelargonidin-3-*O*-malonyl-glucoside-5-*O*-glucoside	Takeda et al. (1986)
a6	2.91	229,277,499	695[M]$^+$(100),595[M-100]$^+$(7),533[M-162]$^+$(34),433[M-(162 + 100)]$^+$(11),271[Y_0]$^+$(48)	Pelargonidin-3-*O*-(6″-*O*-succinyl-glucoside)-5-*O*-glucoside	Takeda et al. (1988)
a7	2.93	247, 276, 517	783[M]$^+$(84),611[M-86-86]$^+$(16),535[M-(162 + 86)]$^+$(72),287[Y_0]$^+$(100)	Cyanidin-3-*O*-malonyl-glucoside-5-*O*-malonyl-glucoside	
a8	3.08	246, 247, 516	797[M]$^+$(100),549[M-(162 + 86)]$^+$(20),535[M-(162 + 100)]$^+$(18),287[Y_0]$^+$(68)	Cyanidin-3-*O*-succinyl-glucoside-5-*O*-malonyl-glucoside	
a9	3.22	239,270,499	767[M]$^+$(100),681[M-86]$^+$(9),595[M-(86 + 86)]$^+$(8),519[M-(162 + 86)]$^+$(10),271[Y_0]$^+$(39)	Pelargonidin-3-*O*-malonyl-glucoside-5-*O*-malonyl-glucoside	Takeda et al. (1986)
a10	3.36	232,285,499	781[M]$^+$(100),695[M-86]$^+$(14),533[M-(162 + 86)]$^+$(12), 519[M-(162 + 100)]$^+$(19),433[M-(162 + 86+100)]$^+$(6),271[Y_0]$^+$(72)	Pelargonidin-3-*O*-malonyl-glucoside-5-*O*-succinyl-glucoside	

1983; Yamaguchi et al., 1995). MS/MS spectrum of **a1** gave a molecular ion at *m/z* 611[M]$^+$ and fragment ion at *m/z* 449[M-162]$^+$, indicating **a1** was a cyanidin derivative with two hexoses, which was subsequently verified as cyanidin-3-*O*-glucoside-5-*O*-glucoside (**Cy3G5G**) by co-elution with a commercial standard. The **a3** molecular ion was *m/z* 86 higher than **a1** with fragment ions at *m/z* 535[M-162]$^+$ and *m/z* 449[M-(162 + 86)]$^+$, which suggested it was a cyanidin glycosylated with two hexoses and acylated with one malonyl acid. Thus, **a3** was putatively identified as cyanidin-3-*O*-malonyl-glucoside-5-*O*-glucoside (**Cy3malonylG5G**). The MS data for **a4** showed a molecular ion at *m/z* 711[M]$^+$ and a major fragment ion at *m/z* 549 [M-162]$^+$. Meanwhile, minority signals at *m/z* 611[M-100]$^+$ and 449[M-(100 + 162)]$^+$ were also detected. Based on previous studies, **a4** was tentatively identified as cyanidin-3-*O*-(6″-*O*-succinyl-glucoside)-5-*O*-glucoside (**Cy3succinylG5G**) (Tamura et al., 1983). The peak **a7** displayed a molecular ion at *m/z* 783[M]$^+$, two fragment ions at *m/z* 611[M-86-86]$^+$ and *m/z* 535[M-(162 + 86)]$^+$ and was identified as cyanidin-3-*O*-malonyl-glucoside-5-*O*-malonyl-glucoside (**Cy3malonylG5malonylG**). The molecular ion at *m/z* 797[M]$^+$ and fragment ions at *m/z* 549[M-(162 + 86)]$^+$ and *m/z* 535[M-(162 + 100)]$^+$, led to the putative identification of **a8** as cyanidin-3-*O*-succinyl-glucoside-5-*O*-malonyl-glucoside (**Cy3succinylG5malonylG**).

Peaks **a2**, **a5**, **a6**, **a9** and **a10**, which shared the maximum absorption at 499 nm and the aglycon ion at *m/z* 271[Y_0]$^+$, were pelargonidin derivatives. Peak **a2** (*m/z* 711 [M]$^+$) was tentatively identified as pelargonidin-3-*O*-malyl-glucoside-5-*O*-glucoside (**Pg3malylG5G**) with fragment ions at *m/z* 595[M-116]$^+$], at *m/z* 549[M-162]$^+$ and *m/z* 433[M-(162 + 116)]$^+$. This was confirmed by the elution profile for **a2**; it eluted 0.38 min earlier than **a5** because malylation shortens the retention time and the electrophoretic mobility when compared with malonylation (Terahara et al., 1986). With the molecular ion at *m/z* 681 [M]$^+$ and fragment ions at *m/z* 595 [M-86]$^+$, *m/z* 519 [M-162]$^+$, *m/z* 433 [M-(86 + 162)]$^+$, compound **a5** putatively matched pelargonidin-3-*O*-malonyl-glucoside-5-*O*-glucoside (**Pg3malonylG5G**). Peak **a6** displayed a molecular ion at *m/z* 695 [M]$^+$ with fragment ions at *m/z* 595 [M-100]$^+$, *m/z* 533 [M-162]$^+$ and *m/z* 433 [M-(100 + 162)]$^+$; this was identified as pelargonidin-3-*O*-(6″-*O*-succinyl-glucoside)-5-*O*-glucoside (**Pg3succinylG5G**) which has been reported for pink cornflower (Takeda et al., 1988). The molecular ion at *m/z* 767 [M]$^+$ in combination with fragment ions at *m/z* 681[M-86], *m/z* 595[M-86-86]$^+$ and *m/z* 519[M-(162 + 86)]$^+$, allowed the tentative identification of **a9** as pelargonidin-3-*O*-malonyl-glucoside-5-*O*-malonyl-glucoside (**Pg3malonylG5malonylG**). The MS data for major peak **a10** (*m/z* 781 [M]$^+$) gave four kinds of fragment ions (*m/z* 695[M-86]$^+$, *m/z* 533[M-(162 + 86)]$^+$, *m/z* 519[M-(162 + 100)]$^+$ and *m/z* 433[M-(162 + 86)-100]$^+$) and was tentatively identified as pelargonidin-3-*O*-malonyl-glucoside-5-*O*-succinyl-glucoside (**Pg3malonylG5succinylG**).

3.3. Identification of flavones and flavonols

There were eight compounds separated using UPLC at 350 nm within 5 min (Fig. 2B). Both positive (PI) and negative (NI) ion mode were chosen for better mass spectrum information. All peaks showed two absorption bands, one in the range of 242–268 nm and the other at 317–347 nm corresponding to bands II and I in the flavonoid spectrum, respectively (Table 3). The putative chemical formulas were shown in Fig. 3B.

The aglycone ions at *m/z* 271[Y_0]$^+$ in PI mode and *m/z* 269[Y_0]$^-$ in NI mode for peaks **f3**, **f4**, **f5** and **f7** indicated they were apigenin derivatives. According to previous studies, glycosylation of apigenins in *Centaurea* often occurred in 7 and 4′ positions (Tamura et al., 1983). **f3** showed a molecular ion at *m/z* 607[M-H]$^-$, fragment ions at *m/z* 445[M-H-162]$^-$ and *m/z* 431[M-H-176]$^-$ in NI mode, and the corresponding ions in PI mode were *m/z* 609[M + H]$^+$, *m/z* 447[M + H-162]$^+$ and *m/z* 433[M + H-176]$^+$ successively; thus **f3** was putatively identified as apigenin-4′-*O*-glucoside-7-*O*-glucuronide (**Ap4′G7Gn**), corresponding

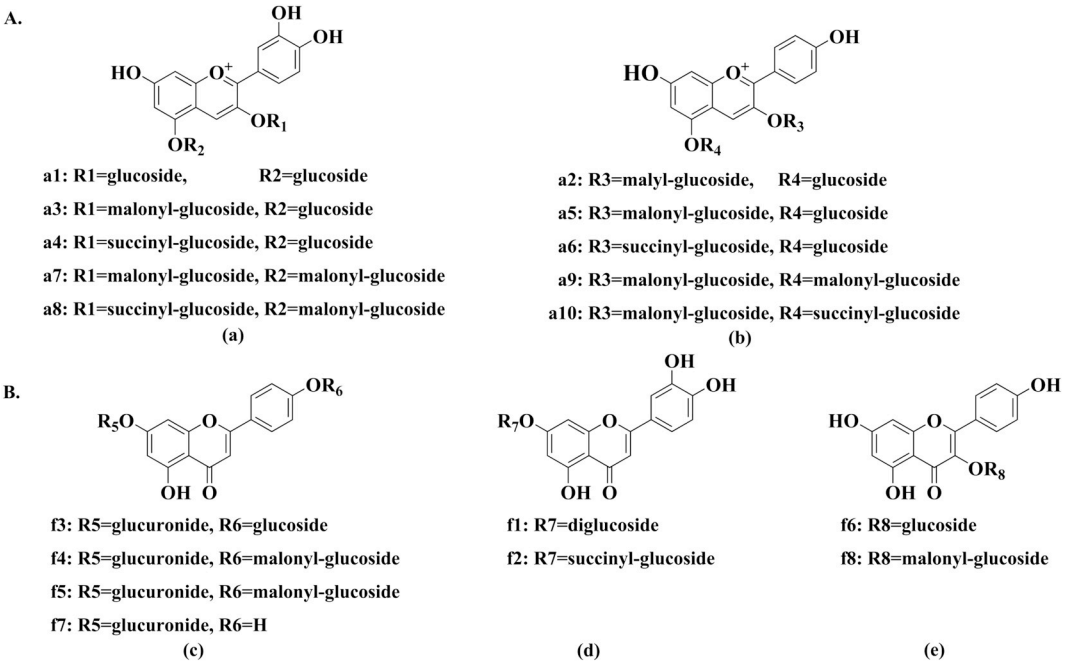

Fig. 3. The putative chemical structure formula of flavonoids in petals of cornflower cultivars. A. anthocyanin. (a) and (b) represent cyanidin and pelargonidin derivatives, respectively. B. Other flavonoids. (c), (d) and (e) represent apigenin, luteolin and kaempferol derivatives, respectively.

to an earlier study (Asen and Horowitz, 1974). **f5** gave molecular ions at *m/z* 695$[M+H]^+$ and *m/z* 693$[M-H]^-$, whose MS^2 spectra showed three fragment ions at *m/z* 609$[M + H\text{-}86]^+$, *m/z* 519$[M + H\text{-}176]^+$(23.3), and *m/z* 447$[M + H\text{-}(162 + 86)]^+$ in PI mode and *m/z* 607$[M\text{-}H\text{-}86]^-$, *m/z* 517$[M\text{-}H\text{-}176]^-$, and *m/z* 445$[M\text{-}H\text{-}(162 + 86)]^-$ in NI mode. This peak was tentatively identified as apigenin-4′-*O*-(6″-*O*-malonyl-glucoside)-7-*O*-glucuronide (**Ap4′malonylG7Gn**), which has been reported as the main flavone in blue cornflower (Tamura et al., 1983). **f4** eluted 0.13 min earlier than **f5** and shared similar UV absorption characteristics and ion pattern with **f5**. Thus, **f4** was assigned as the isomer of **f5**, and the distinct retention times may be caused by variation in the position of the glucuronide or malonylglucoside. The molecular ions at *m/z* 447$[M+H]^+$ and *m/z* 445$[M\text{-}H]^-$ in PI and NI mode, respectively, led to the tentative identification of **f7** as apigenin-7-*O*-glucuronide (**Ap7Gn**), which was also found in other cyanic-flowered *Centaurea* species, such as *C. achtarovii*, *C. dealbata* and *C. montana* (Mishio et al., 2015).

Peaks **f1**, **f2**, **f6** and **f8** were considered to be kaempferol or luteolin with aglycone ions at *m/z* 287$[Y_0]^+$ and *m/z* 285$[Y_0]^-$. Subsequently, **f6** and **f8** were verified as kaempferol according to the location of band II at 265 nm (Markham, 1982), and **f1** and **f2** were identified as luteolin based on the location of band II around 245 nm. In plants of the composite family, the glycosylation of luteolin often occurred at the 7 position (Lin and Harnly, 2010; Mishio et al., 2015). The molecular ion at *m/z* 611$[M+H]^+$ and *m/z* 609$[M\text{-}H]^-$ in **f1** gave fragment ions at *m/z* 449$[M + H\text{-}162]^+$ and *m/z* 447$[M\text{-}H\text{-}162]^-$ respectively, thus **f1** was putatively identified as luteolin-7-*O*-diglucoside (**Lu7diG**). The *m/z* 449$[M + H\text{-}100]^+$ and *m/z* 447$[M + H\text{-}100]^-$ were the fragment ions of *m/z* 549$[M+H]^+$ and *m/z* 547$[M\text{-}H]^-$, respectively, thus **f2** was tentatively identified as luteolin-7-*O*-succinyl-glucoside (**Lu7succinylG**). Peak **f6** was considered as kaempferol-3-*O*-glucoside (**Ka3G**) with molecular ions at *m/z* 449$[M+H]^+$ and *m/z* 447$[M\text{-}H]^-$. **f8** was 86 units greater than **f6**, which corresponded to a loss of the malonyl unit; thus, **f8** was tentatively identified as kaempferol-3-*O*-malonyl-glucoside (**Ka3malonylG**).

3.4. Flavonoid content among cornflower cultivars

The flavonoid composition as well as content varied significantly among cultivars (Table 4). There were diverse anthocyanins detected in five cultivars but not DTPW. Cy3succinylG5G and Pg3succinylG5G were the only anthocyanins detected in DTPB and DTPP, respectively. The pelargonidin derivatives in DTPR showed abundant glycosylation and acylation, in which Pg3malonylG5G and Pg3succinylG5G accounted for 80.5 percent of total anthocyanin content. Cy3succinylG5G was the main anthocyanin (78 percent) in TDBM. There were five cyanidin derivatives acylated with different aliphatic acids in TDBB, in which Cy3malonylG5G and Cy3succinylG5G accounted for 40.7 and 36.8 percent, respectively. There were also other flavonoids detected in petals of cornflower cultivars. Ap4′malonylG7Gn was the main flavone detected in DTPW, DTPB and DTPP at the percentage of 67.9, 86.5 and 82.8, respectively. The main flavone in DTPR and TDBM was Ap7Gn, whereas Lu7diG, Lu7succinylG and Ap4′malonylG7G were at 68 percent in TDBB. Interestingly, the petals of DTPB, TDBM and TDBB all contained cyanidin derivatives but revealed visibly different colours. After comparing the content ratios of total flavones and flavonols to total anthocyanins, we found the ratios in DTPB and TDBM were all greater than 1.5. However, the ratio in TDBB was less than 0.5 because the content of anthocyanin in TDBB was dominant over other flavonoids. Therefore, we speculated the hyper-accumulation of cyanidin derivatives was responsible for the black coloration.

3.5. The expression and sequence analysis of genes involved in flavonoid biosynthesis

In order to explore the potential molecular mechanism of flavonoid biosynthesis branch pathway in cornflower, the expression patterns of seventeen key structural genes obtained from transcriptome (unpublished), including one each of *PAL*, 4CL, *FNS*, *F3H*, *F3′H*, *DFR* and *ANS*, two each of *CHI* and *AT*, and three each of *CHS* and *GT* were

Table 3
Putative identification of flavones and flavonols in petals of cornflower cultivars by I-Class UPLC/XevoTM TQ MS.

Peak No.	Tr(min)	λ_{max}(nm)	ESI(+)	ESI(-)	Putative identification	References
f1	2.19	242, 335	611$[M+H]^+$(10),449[M + H-162]$^+$(10), 287$[Y_0]^+$(90)	609$[M-H]^-$(4),447[M-H-162]$^-$(9), 285$[Y_0]^-$(91)	Luteolin-7-*O*-diglucoside	
f2	2.32	245, 336	549$[M+H]^+$(18),449[M + H-100]$^+$(1), 287$[Y_0]^+$(43)	547$[M-H]^-$(13),447[M-H-100]$^-$(68), 285$[Y_0]^-$(75)	Luteolin-7-*O*-succinyl-glucoside	
f3	3.21	268, 317	609$[M+H]^+$(100),447[M + H-162]$^+$(2),433[M + H-176]$^+$(20),271$[Y_0]^+$(23)	607$[M-H]^-$(100),445[M-H-162]$^-$(6),431[M-H-176]$^-$(79),269$[Y_0]^-$(63)	Apigenin-4′-*O*-glucoside-7-*O*-glucuronide	Asen and Horowitz (1974)
f4	3.64	268, 318	695$[M+H]^+$(100),519[M + H-176]$^+$(10.3), 447[M + H-(162 + 86)]$^+$(7.1), 271$[Y_0]^+$(24.6)	517[M-H-176]$^-$(21.9),445[M-H-(162 + 86)]$^-$(51.5),269$[Y_0]^-$(94.4),268$[Y_0$-H]$^-$(1.9)	Apigenin-4′-*O*-(6″-*O*-malonyl-glucoside)-7-*O*-glucuronide (isomer)	
f5	3.77	268,319	695$[M+H]^+$(100),609[M + H-86]$^+$(2.1), 519[M + H-176]$^+$(23.3),447[M + H-(162 + 86)]$^+$(3.7),271$[Y_0]^+$(39.4)	693$[M-H]^-$(100),607[M-H-86]$^-$(3.0), 517[M-H-176]$^-$(16.1),445[M-H-(162 + 86)]$^-$(7.4),269$[Y_0]^-$(26.9),268$[Y_0$-H]$^-$(4.7)	Apigenin-4′-*O*-(6″-*O*-malonyl-glucoside)-7-*O*-glucuronide	Tamura et al. (1983)
f6	4.29	265,347	449$[M+H]^+$(2.5),287$[Y_0]^+$(100)	447$[M-H]^-$(100),285$[Y_0]^-$(38.5), 284$[Y_0$-H]$^-$(27.8)	Kaempferol-3-*O*-glucoside	Lockowandt et al. (2019)
f7	4.45	266,336	447$[M+H]^+$(28.4),271$[Y_0]^+$(100)	445$[M-H]^-$(100),269$[Y_0]^-$(45.9), 268$[Y_0$-H]$^-$(0.27),	Apigenin-7-*O*-glucuronide	Mishio et al. (2015)
f8	4.55	265,347	535$[M+H]^+$(4.4),449[M + H-86]$^+$(2.0), 287$[Y_0]^+$(100)	533$[M-H]^-$(7.3),447[M-H-86]$^-$(3.1), 285$[Y_0]^-$(100),284$[Y_0$-H]$^-$(31.6)	Kaempferol-3-*O*-malonyl-glucoside	

Table 4
The flavonoid contents in petals of different cornflower cultivars mg·g^{-1}(dry weight).

Peak No.	Flavonoid	Cultivars					
		DTPW	DTPP	DTPR	DTPB	TDBM	TDBB
a1	Cy3G5G	-	-	-	-	0.71 ± 0.03	7.86 ± 2.56
a2	Pg3malylG5G	-	-	3.96 ± 0.70	-	-	-
a3	Cy3malonylG5G	-	-	-	-	0.68 ± 0.13	24.81 ± 8.18
a4	Cy3succinylG5G	-	-	-	8.31 ± 0.17	4.82 ± 0.89	22.42 ± 2.46
a5	Pg3malonylG5G	-	-	12.77 ± 2.21	-	-	-
a6	Pg3succinylG5G	-	2.45 ± 0.02	11.20 ± 1.97	-	-	-
a7	Cy3malonylG5malonylG	-	-	-	-	-	2.60 ± 0.85
a8	Cy3succinylG5malonylG	-	-	-	-	-	3.23 ± 0.67
a9	PgmalonylG5malonylG	-	-	0.68 ± 0.15	-	-	-
a10	Pg3malonylG5succinylG	-	-	0.65 ± 0.15	-	-	-
f1	Lu7diG	-	-	-	-	-	5.99 ± 2.20
f2	Lu7succinylG	-	-	-	-	1.51 ± 0.35	7.22 ± 0.90
f3	Ap4′G7Gn	0.44 ± 0.09	1.14 ± 0.01	-	0.25 ± 0.04	-	2.03 ± 0.88
f4	f5 isomer	0.42 ± 0.07	0.71 ± 0.00	-	0.01 ± 0.00	-	0.29 ± 0.09
f5	Ap4′malonylG7Gn	15.77 ± 1.40	21.36 ± 0.07	-	13.02 ± 1.25	-	6.05 ± 2.36
f6	Ka3G	-	-	1.25 ± 0.31	-	0.10 ± 0.04	-
f7	Ap7Gn	-	-	32.83 ± 5.52	-	21.41 ± 2.57	3.40 ± 0.10
f8	Ka3malonylG	-	0.18 ± 0.01	3.30 ± 0.66	-	-	-
TA	-	0	2.45 ± 0.02	29.3 ± 5.2	8.31 ± 0.17	6.2 ± 1.0	61.0 ± 10.9
TF	-	16.6 ± 1.6	23.4 ± 0.1	37.4 ± 6.5	13.1 ± 1.5	23.0 ± 3.0	22.4 ± 4.3
TF/TA	-	∞	9.5 ± 0.1	1.3 ± 0.0	1.6 ± 0.1	3.7 ± 0.16	0.4 ± 0.0

TF represents total flavone and flavonol content, TA represents total anthocyanin content, and their relative content was shown by TF/TA.

analysed (Fig. 4). The flavone synthesis gene, *FNS*, reached maximum expression in the first stage and the expression decreased gradually in the following stages. The anthocyanin biosynthesis in DTPW was blocked starting from *F3H*, which explained the absence of anthocyanin. Apart from *FNS*, the expression level of most structural genes in DTPP, DTPB and TDBM were highest during stage 2 or 3, whereas that case in DTPR and TDBB were rising continually throughout the development process; this corresponded with their hyper-accumulation of flavonoids (Fig. 4). Although there were only pelargonidin derivatives detected in DTPP and DTPR, the expression levels of *F3′H* were relatively high. Therefore, we performed the sequence analysis of two key genes that may control the biosynthesis of the pelargonidin and cyanidin branch pathway. By multiple sequence alignment of *DFR* from five cultivars accumulating anthocyanins, we found the sequence of *DFR* was highly conserved among cultivars with high sequence similarity up to 100 percent (Fig. S1), which suggested the *DFR* in cornflower showed no substrate specificity. Furthermore, the *F3′H* in DTPB, TDBM and TDBB that accumulated cyanidin derivatives was 1545 bp and contained the *F3′H* specific motif of LPPGP, VVVAASAS and the CYP450 conserved motifs of oxygen-binding site (OBS) and haem-binding site (HBS). However, the *F3′H* was truncated to 1059 bp in cultivars accumulating pelargonidin derivatives (DTPP and DTPR), losing the key motif of HBS, where the normal ability to convert DHK to DHQ may be lost at the same time (Fig. 5). Notably, the expression level of *GT1* was only detected in DTPB, TDBM and TDBB and not in DTPP and DTPR. Therefore, we deduced that this enzyme may possess substrate specificity and only catalysed the glycosylation of cyanidin. Because the expression trends of *GT3* and *AT2* were consistent with *FNS*, we speculated they may catalyse the glycosylation and acylation of flavone in cornflowers, respectively.

4. Discussion

In the present study, we collected six *C. cyanus* cultivars with obviously different colours. The UPLC-MS/MS was applied to analyse flavonoids both qualitatively and quantitatively. In total, there were ten anthocyanins, six flavones and two flavonols isolated and putatively identified. Different from *Senecio cruentus* and *Muscari* with delphinidin, pelargonidin and cyanidin derivatives coexisting in the same petal (Jin et al., 2016; Lou et al., 2017), the anthocyanin-type in *C. cyanus* is relatively simple; there were only cyanidins detected in blue, mauve and black petals, and pelargonidins in pink and red cultivars. Although the pink and red flowers both belonged to the red-purple group according to the RHSCC, their L^*, a^* and C values showed significant differences. Further chemical analysis found the pelargonidin derivatives were more abundant in red petals. The pink petals accumulated only Pg3succinylG5G whereas the red contained five cyanidins with more diversified modifications. The total flavonoid content of red petals was almost three times higher than that in the pink petals, which may result in the different coloration.

Upon consideration of the flower colour phenotype and anthocyanin composition results, it was apparent that blue flower colour development happened only when cyanidin was present in cornflower. Shiono et al. (2005) verified the crystal structure of protocyanin in the blue cornflower by X-ray as a supramolecular pigment composed of six molecules each of anthocyanin and flavone, one ferric iron, one magnesium and two calcium ions. The metal ions coordinated with *ortho*-dihydroxy groups, thus the chromophore must contain at least two free hydroxyl groups on the B-ring for chelating metal ions (Sigurdson et al., 2016). Therefore, the pelargonidin with only one hydroxy on the B-ring could not form metalloanthocyanin with metal ions. Interestingly, the mauve and black petals both accumulated cyanidin derivatives but still did not develop the vivid blue colour. We found both the blue and mauve cornflower accumulated the same anthocyanin, Cy3succinylG5G, whereas the flavone in the blue and mauve flower was Ap4′-malonylG7Gn and Ap7Gn, respectively; this is different from the early study that both the blue cornflower and its mauve mutant accumulated the same flavonoids (Yoshida and Negishi., 2013). The previous studies have provided evidence of the great role that glucosylation played in blue colour development. For example, the original blue petals of *Lobelia erinus* changed to be mauve after the loss of rhamnosylation in delphinidin 3-*O*-glucoside, and the mauve plants transformed with the functional rhamnosyltransferase produced blue flowers again (Hsu et al., 2017). The ray flowers of *Chrysanthemum* × *morifolium* transformed with exogenous *F3′5′H* gene accumulated delphidin 3-*O*-(6″-*O*-malonyl)glucoside and exhibited only violet colour, whereas further glucosylations of the 3′ and 5′ positions on the B-ring of delphinidin later transformed with anthocyanin 3′,5′-*O*-glucosyltransferase gene

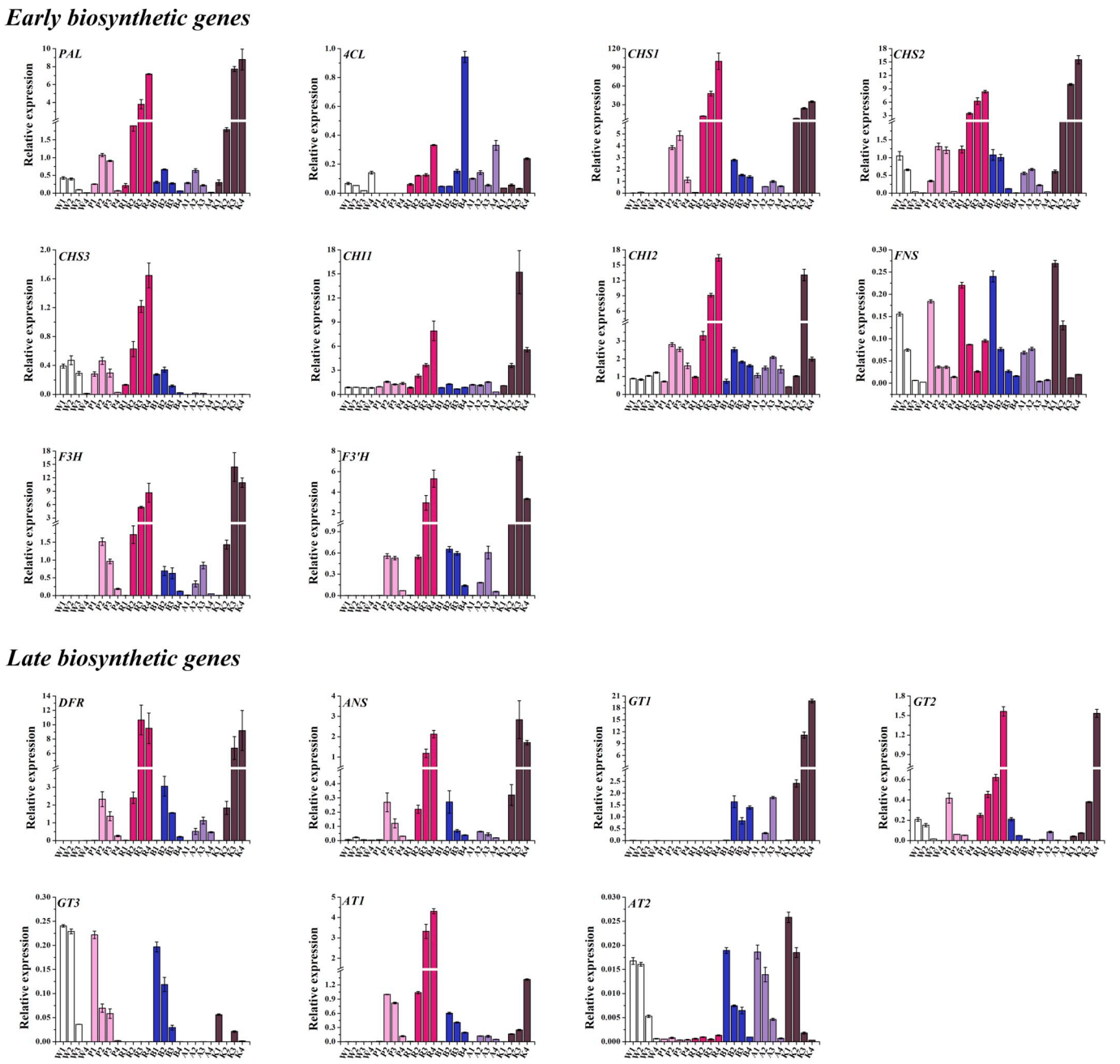

Fig. 4. The expression patterns of genes involved in flavonoid biosynthetic pathway among cornflower cultivars and their developmental stages. phenylalanine ammonia lyase(*PAL*), 4-coumarate: CoA ligase(4CL), chalcone synthase(*CHS*), chalcone isomerase(*CHI*), flavanone-3-hydroxylase(*F3H*), flavonoid 3′-hydroxylase (*F3′H*), dihydroflavonol 4-reductase(*DFR*), anthocyanidin synthase(*ANS*), flavonoid glucosyltransferase(*GT*), acyltransferase(*AT*). The column colours were consistent with cornflower petals, and developmental stages were divided in 2.1. (For interpretation of the references to colour in this figure legend, the reader is referred to the Web version of this article.)

produced blue colour through intermolecular association with flavone derivatives (Noda et al., 2013 & 2017). By transcriptome analysis, Wu et al. (2016) found glucosyltransferase *UA3GTs*, were the most important candidates that induced blue petal colour formation in Nymphaea 'King of Siam'. These results illustrated that the flavonoid glucosylation may be involved in blue colour development. Therefore, we speculated the glucosylation of the 4′ position on the apigenin aglycone played an important role in the generation of the blue supramolecular pigment. The Ap7Gn may not generate a stable pigment complex, which finally led to the mauve coloration. In the black cornflower, there were five cyanidin derivatives acylated with various acids, whose total content was as high as 61 mg/g (dry weight), at least 8 times greater than that in blue and mauve flowers. Therefore, the black coloration in cornflower may be attributed to the hyper-accumulation of cyanidin derivatives, similar to black *Dahlia variabilis* petals (Deguchi et al., 2016).

Acylation occurs widely in plant flavonoids, and the acids involved in this process include aliphatic and aromatic acids. The acylation sites, types and numbers of acyl groups have effects on the stability of anthocyanins (Zhao et al., 2017). The previous study showed anthocyanins acylated with aromatic acids typically generate a stable blue colour. For example, the blue petals of *Senecio cruentus*, *Gentiana*, *Delphinium* and *Lobelia erinus* all accumulated anthocyanins polyacylated with aromatic acids (Nakatsuka et al., 2010; Miyagawa et al., 2015; Hsu

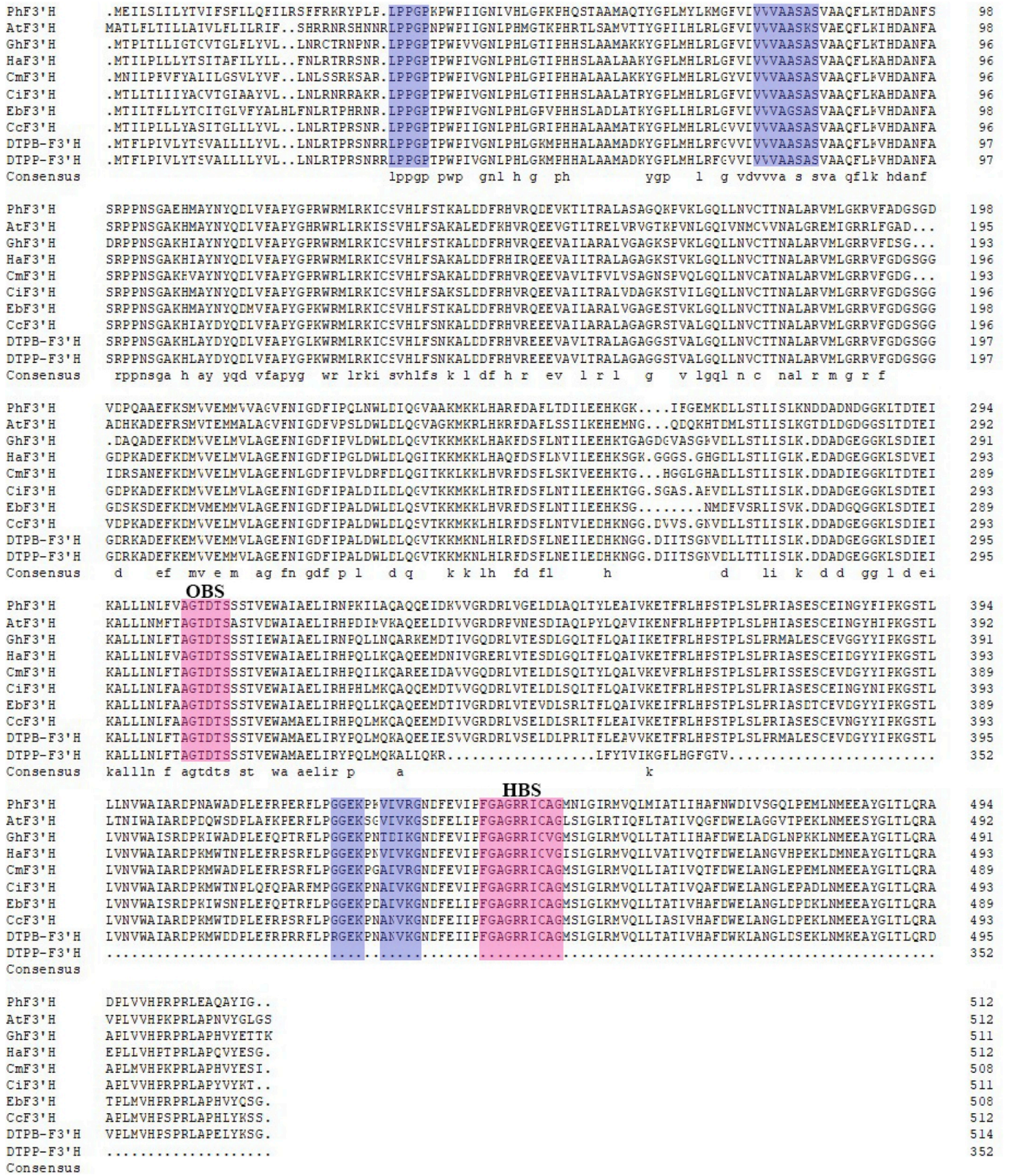

Fig. 5. The multiple alignment of *F3′H* from different species. The blue rectangles were specific motifs of *F3′H*, and the red rectangles were conserved motifs of CYP450 family. *AtF3′H*(*Arabidopsis thaliana*, 4AF271651);*HaF3′H*(*Helianthus annuus*, XP_021978269);*GhF3′H*(*Gerbera hybrid*, ABA64468);*CmF3′H*(*Chrysanthemum* × *morifolium*, ADA85882);*EbF3′H*(*Echinops bannaticus*, ACN65826);*CiF3′H*(*Cichorium intybus*, ACN65825);*CcF3′H*(*Cynara cardunculus var. scolymus*, ADM26615);*PhF3′H*(*Petunia* × *hybrida*, Q9SBQ9). (For interpretation of the references to colour in this figure legend, the reader is referred to the Web version of this article.)

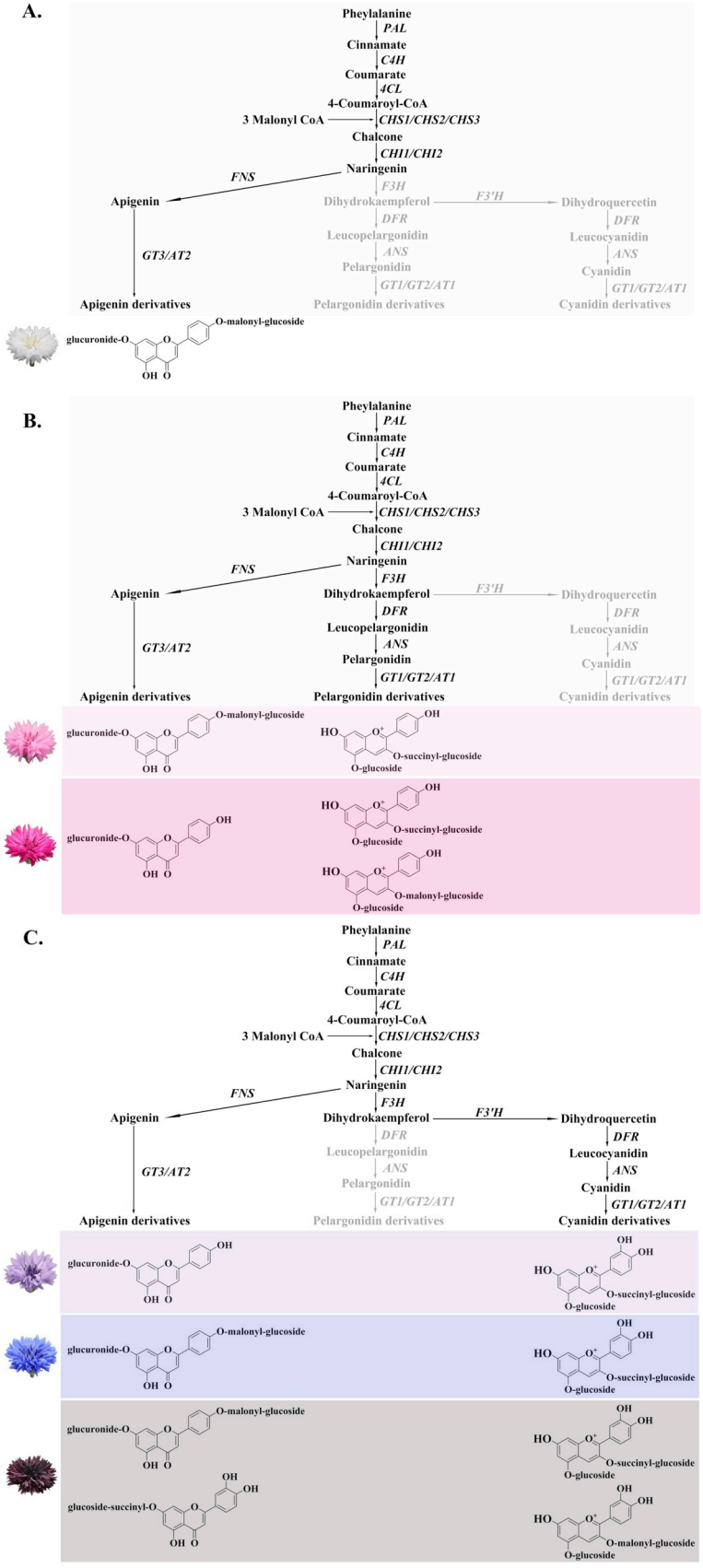

Fig. 6. The flavonoid biosynthetic pathway in DTPW(A), DTPP and DTPR(B), DTPB, TDBM and TDBB(C). The chemical formulas of flavonoids mainly accumulated in petals of six cornflower cultivars were also shown after the biosynthetic pathway.

et al., 2017). However, acylation with fatty acids did not change flower colour but increase the stability and solubility of flavonoids (Zhao et al., 2017). Using UPLC-MS/MS, we found the flavonoids in cornflower petals were widely acylated with fatty acids, such as malonic, succinic and malic acids. The succinate ester of cyanidin was characteristic in the genus of *Centaurea* (Sulyok and László-Bencsik, 1985). Yamaguchi et al. (1995) found the acyltransferase in cornflower catalysed the transfer of the succinyl moiety from succinyl-CoA to 3-*O*-glucosides of cyanidin by in vitro enzyme assays, while it also catalysed the malonylation of cyanidin. The concrete role of flavonoid acylation in cornflower coloration has yet to be determined.

Flavonoid compositions play a key role in coloration. We further examined the expressional level of structural genes and deduced the flavonoid biosynthetic pathway to gain a more global view of the molecular mechanism of petal colour variation in cornflower cultivars (Fig. 6). The results showed the anthocyanin biosynthetic pathway in DTPW was blocked starting from *F3H*, which may be caused by the loss of the *MYB-bHLH-WD40* complex. In *Lilium speciosum*, an amino acid substitution on the R2 repeat of *LsMYB12* resulted in decreased anthocyanin biosynthetic gene transcription and no tepal pigmentation (Suzuki et al., 2015). The *MYBL1* in *Iochroma loxense*, a *MYB* transcriptional repressors, was associated with downregulation of multiple anthocyanin pigment pathway genes and responsible for the conversion to white flowers (Gates et al., 2018). The white flower in *S. cruentus* and *Dianthus* originated from the absence of *bHLH* expression (Jin et al., 2016; Totsuka et al., 2018). The anthocyanin type in cornflower is relatively simple; the petals can generate only one kind of anthocyanidin, either cyanidin in DTPB, TDBM and TDBB or pelargonidin in DTPP and DTPR. The *F3′H* and *DFR* genes played an important role in controlling the biosynthetic pathway to cyanidin or pelargonidin flux. The important enzyme *DFR*, which catalysed dihydroflavonol to leucoanthocyanidin, showed substrate specificity in many species, such as that seen in *Freesia hybrida* and *Petunia hybrida* (Li et al., 2017; Johnson et al., 2001). In contrast, we found the *DFR* sequences in different cornflower cultivars were completely the same, where no substrate specificity occurred. The *F3′H* enzyme belonging to the cytochrome P450 is an essential part for the introduction of a second hydroxy group in the B-ring of flavonoids, catalysing DHK to DHQ. We found that a mutation occurred in the open reading frame of *F3′H* in DTPP and DTPR, accumulating only pelargonins, losing the key motif of the haem binding site of CYP450, which may result in the loss of DHK to DHQ conversion. In *Ipomoea* species, the nonsense mutation by a single base insertion or transposon insertion of *F3′H* conferred reddish rather than blue flowers (Hoshino et al., 2003). The rare orange-red poinsettia was also caused by the nonsense mutation in *F3′H* (Nitarska et al., 2018). Interestingly, hyperaccumulation of cyanidin derivatives in the black cultivar TDBB showed apparently high expression levels of genes when compared with DTPB and TDBM in the anthocyanin biosynthetic pathway. According to black *Dahlia variabilis*, the suppression of *DvFNS* caused by small RNA abolished the competition between anthocyanidin and flavone synthesis, thus leading to the hyper-accumulation of cyanidin (Deguchi et al., 2016). Whereas the apigenin and luteolin were highly coexisting with cyanidin derivatives in TDBB. The question remains why most of the naringenins flow to the branch pathway of cyanidin synthesis in black petals.

5. Conclusions

In the present study, the flavonoids in petals of six *C. cyanus* cultivars with visibly different colours were qualitatively and quantitatively examined using UPLC-MS/MS. There were eighteen compounds isolated and tentatively identified, including ten anthocyanins, six flavones and two flavonols, which were widely acylated with aliphatic acids. The compositions and contents of flavonoids varied among cultivars. The anthocyanin biosynthesis in white cultivars was blocked starting from *F3H*, which resulted in the absence of anthocyanin accumulation. The pink and red cornflowers could only accumulate pelargonidin derivatives caused by the mutation of *F3′H*. Within the cyanidin accumulators (the blue, mauve and black cultivars), the relative content of total anthocyanin to total flavone and flavonol played an important role in colour generation among the three cultivars. The results presented above will improve our understanding of the chemical basis and molecular mechanism for colour diversity in *C. cyanus*.

Silan Dai and Liangsheng Wang conceived the experiments and edited the paper; Shanshan Li, Chengyong Feng and Chengyan Deng performed the UPLC-MS/MS analysis; Chengyan Deng and Jiaying Wang performed gene expression and sequence analysis; Chengyan Deng, He Huang and Yan Hong analysed the data; Chengyan Deng wrote the paper.

Conflicts of interest

The authors hereby declare no conflicts of interests.

Acknowledgements

This research was supported by the National Key Research and Development Program (2018YFD1000405).

Appendix A. Supplementary data

Supplementary data to this article can be found online at https://doi.org/10.1016/j.plaphy.2019.06.018.

Author contributions

Silan Dai and Liangsheng Wang conceived the experiments and edited the paper;

Shanshan Li, Chengyong Feng and Chengyan Deng performed the UPLC-MS/MS analysis;

Chengyan Deng and Jiaying Wang performed gene expression and sequence analysis;

Chengyan Deng, He Huang and Yan Hong analysed the data;

Chengyan Deng wrote the paper.

References

Asen, S., Horowitz, R.M., 1974. Apigenin 4′-*O*-*β*-D-glucoside 7-*O*-*β*-D)-glucuronide: the copigment in the blue pigment of *Centaurea cyanus*. Phytochemistry 13, 1219–1223.

Deguchi, A., Tatsuzawa, F., Hosokawa, M., Doi, M., Ohno, S., 2016. Quantitative evaluation of the contribution of four major anthocyanins to black flower coloring of Dahlia petals. Hortic. J. 85, 340–350.

Gates, D.J., Olson, B.J.S.C., Clemente, T.E., Smith, S.D., 2018. A novel R3 MYB transcriptional repressor associated with the loss of floral pigmentation in Iochroma. New Phytol. 217 (3), 1346–1356.

Haselmair-Gosch, C., Miosic, S., Nitarska, D., Roth, B.L., Walliser, B., Paltram, R., Lucaciu, R.C., Eidenberger, L., Rattei, T., Olbricht, K., Stich, K., Halbwirth, H., 2018. Great cause—small effect: undeclared genetically engineered orange petunias harbor an inefficient dihydroflavonol 4-reductase. Front. Plant Sci. 9, 1–12.

Hong, Y., Tang, X., Huang, H., Zhang, Y., Dai, S., 2015. Transcriptomic analyses reveal species-specific light-induced anthocyanin biosynthesis in chrysanthemum. BMC Genomics 16, 1–18.

Hoshino, A., Morita, Y., Choi, J.D., Saito, N., Toki, K., Tanaka, Y., Iida, S., 2003. Spontaneous Mutations of the flavonoid 3′-hydroxylase gene conferring reddish flowers in the three morning glory species. Plant Cell Physiol. 44, 990–1001.

Hsu, Y.H., Tagami, T., Matsunaga, K., Okuyama, M., Suzuki, T., Noda, N., Suzuki, M., Shimura, H., 2017. Functional characterization of UDP-rhamnose-dependent rhamnosyltransferase involved in anthocyanin modification, a key enzyme determining blue coloration in Lobelia erinus. Plant J. 89, 325–337.

Ishii, I., Sakaguchi, K., Fujita, K., Ozeki, Y., Miyahara, T., 2017. A double knockout mutant of acyl-glucose-dependent anthocyanin glucosyltransferase genes in *Delphinium grandiflorum*. J. Plant Physiol. 216, 74–78.

Jin, X., Huang, H., Wang, L., Sun, Y., Dai, S., 2016. Transcriptomics and metabolite analysis reveals the molecular mechanism of anthocyanin biosynthesis branch pathway in different *Senecio cruentus* cultivars. Front. Plant Sci. 7, 1–14.

Johnson, E.T., Ryu, S., Yi, H., Shin, B., Cheong, H., Choi, G., 2001. Alteration of a single amino acid changes the substrate specificity of dihydroflavonol 4-reductase. Plant J. 25, 325–333.

Li, P., Li, Y.J., Zhang, F.J., Zhang, G.Z., Jiang, X.Y., Yu, H.M., Hou, B.K., 2017. The

Arabidopsis UDP-glycosyltransferases UGT79B2 and UGT79B3, contribute to cold, salt and drought stress tolerance via modulating anthocyanin accumulation. Plant J. 89, 85–103.
Li, Y., Liu, X., Cai, X., Shan, X., Gao, R., Yang, S., Han, T., Wang, S., Wang, L., Gao, X., 2017. Dihydroflavonol 4-reductase genes from *Freesia hybrida* play important and partially overlapping roles in the biosynthesis of flavonoids. Front. Plant Sci. 8, 1–15.
Lin, L.Z., Harnly, J.M., 2010. Identification of the phenolic components of chrysanthemum flower (*Chrysanthemum morifolium* Ramat). Food Chem. 120, 319–326.
Lockowandt, L., Pinela, J., Roriz, C.L., Pereira, C., Abreu, R.M.V., Calhelha, R.C., Alves, M.J., Barros, L., Bredol, M., Ferreira, I.C.F.R., 2019. Chemical features and bioactivities of cornflower (Centaurea cyanus L.) capitula: the blue flowers and the unexplored non-edible part. Ind. Crops Prod. 128, 496–503.
Lotkowska, M.E., Tohge, T., Fernie, A.R., Xue, G.-P., Balazadeh, S., Mueller-Roeber, B., 2015. The Arabidopsis transcription factor MYB112 promotes anthocyanin formation during salinity and under high light stress. Plant Physiol. 169, 1862–1880.
Lou, Q., Wang, L., Liu, H., Liu, Y., 2017. Anthocyanin profiles in flowers of grape hyacinth. Molecules 22, 1–9.
Markham, K.R., 1982. Techniques of Flavonoid Identification, first ed. Academic Press, London.
Mishio, T., Takeda, K., Iwashina, T., 2015. Anthocyanins and other flavonoids as flower pigments from eleven *Centaurea* species. Nat Prod Commun 10 (3), 447–450.
Miyagawa, N., Miyahara, T., Okamoto, M., Hirose, Y., Sakaguchi, K., Hatano, S., Ozeki, Y., 2015. Dihydroflavonol 4-reductase activity is associated with the intensity of flower colors in delphinium. Plant Biotechnol. 32, 249–255.
Nakatsuka, T., Mishiba, K., Kubota, A., Abe, Y., Yamamura, S., Nakamura, N., Tanaka, Y., Nishihara, M., 2010. Genetic engineering of novel flower colour by suppression of anthocyanin modification genes in gentian. J. Plant Physiol. 167, 231–237.
Nitarska, D., Stefanini, C., Haselmair-Gosch, C., Miosic, S., Walliser, B., Mikulic-Petkovsek, M., Regos, I., Slatnar, A., Debener, T., Terefe-Ayana, D., Vilperte, V., Hadersdorfer, J., Stich, K., Halbwirth, H., 2018. The rare orange-red colored Euphorbia pulcherrima cultivar “Harvest Orange” shows a nonsense mutation in a flavonoid 3’-hydroxylase allele expressed in the bracts. BMC Plant Biol. 18, 1–12.
Noda, N., Aida, R., Kishimoto, S., Ishiguro, K., Fukuchi-Mizutani, M., Tanaka, Y., Ohmiya, A., 2013. Genetic engineering of novel bluer-colored chrysanthemums produced by accumulation of delphinidin-based anthocyaninsx. Plant Cell Physiol. 54, 1684–1695.
Noda, N., Yoshioka, S., Kishimoto, S., Nakayama, M., Douzono, M., Tanaka, Y., Aida, R., 2017. Generation of blue chrysanthemums by anthocyanin B-ring hydroxylation and glucosylation and its coloration mechanism. Sci. Adv. 3, 1–10.
Shiono, M., Matsugaki, N., Takeda, K., 2005. Structure of the blue cornflower pigment. Nature 436 791–791.
Sigurdson, G.T., Robbins, R.J., Collins, T.M., Giusti, M.M., 2016. Evaluating the role of metal ions in the bathochromic and hyperchromic responses of cyanidin derivatives in acidic and alkaline pH. Food Chem. 208, 26–34.
Sulyok, G., László-Bencsik, Á., 1985. Cyanidin 3-(6-succinyl glucoside)-5-glucoside from flowers of seven *Centaurea* species. Phytochemistry 24 (5), 1121–1122.
Suzuki, K., Suzuki, T., Nakatsuka, T., Dohra, H., Yamagishi, M., Matsuyama, K., Matsuura, H., 2016. RNA-seq-based evaluation of bicolor tepal pigmentation in Asiatic hybrid lilies (*Lilium* spp.). BMC Genomics 17, 1–19.
Suzuki, K., Tasaki, K., Yamagishi, M., 2015. Two distinct spontaneous mutations involved in white flower development in *Lilium speciosum*. Mol. Breed. 35, 1–14.
Takeda, K., Harborne, J.B., Self, R., 1986. Identification and distribution of malonated anthocyanins in plants of the compositae. Phytochemistry 25, 1337–1342.
Takeda, K., Kumegawa, C., Harborne, J.B., Self, R., 1988. Pelargonidin 3-(6"-succinyl glucoside)-5-glucoside from pink *Centaurea cyanus* flowers. Phytochemistry 27 (4), 1228–1229.
Tamura, H., Kondo, T., Kato, Y., Goto, T., 1983. Structures of a succinyl anthocyanin and a malonyl flavone, two constituents of the complex blue pigment of cornflower *Centaurea cyanus*. Tetrahedron Lett. 24 (51), 5749–5752.
Terahara, N., Yamaguchi, M., Takeda, K., Harborne, J.B., Self, R., 1986. Anthocyanins acylated with malic acid in *Dianthus caryophyllus* and *D. deltoides*. Phytochemistry 25 (7), 1715–1717.
Tohge, T., De Souza, L.P., Fernie, A.R., 2017. Current understanding of the pathways of flavonoid biosynthesis in model and crop plants. J. Exp. Bot. 68, 4013–4028.
Totsuka, A., Okamoto, E., Miyahara, T., Kouno, T., Cano, E.A., Sasaki, N., Watanabe, A., Tasaki, K., Nishihara, M., Ozeki, Y., 2018. Repressed expression of a gene for a basic helix-loop-helix protein causes a white flower phenotype in carnation. Breed Sci. 68, 139–143.
Wu, Q., Wu, J., Li, S.S., Zhang, H.J., Feng, C.Y., Yin, D.D., Wu, R.Y., Wang, L.S., 2016. Transcriptome sequencing and metabolite analysis for revealing the blue flower formation in waterlily. BMC Genomics 17, 1–13.
Yamaguchi, M., Maki, T., Ohishi, T., Ino, I., 1995. Succinyl-coenzyme A: anthocyanidin 3-glucoside succinyltransferase in flowers of *Centaurea cyanus*. Phytochemistry 39, 311–313.
Yoshida, K., Kitahara, S., Ito, D., Kondo, T., 2006. Ferric ions involved in the flower color development of the Himalayan blue poppy, Meconopsis grandis. Phytochemistry 67, 992–998.
Yoshida, K., Negishi, T., 2013. The identification of a vacuolar iron transporter involved in the blue coloration of cornflower petals. Phytochemistry 94, 60–67.
Zhao, D., Tao, J., 2015. Recent advances on the development and regulation of flower color in ornamental plants. Front. Plant Sci. 6, 1–13.
Zhao, C.L., Yu, Y.Q., Chen, Z.J., Wen, G.S., Wei, F.G., Zheng, Q., Wang, C. De, Xiao, X.L., 2017. Stability-increasing effects of anthocyanin glycosyl acylation. Food Chem. 214, 119–128.